A THESIS FOR THE DEGREE OF MASTER OF SCIENCE

Effect of Growth Progress on Positional Distribution of UV-B Light Interception and Bioactive Compound Contents in Kale

생육진전이 케일의 수광 및 생활성 화합물의 위치적 분포에 미치는 영향

BY

HYUN YOUNG KIM

FEBURARY, 2021

MAJOR IN HORTICULTURAL SCIENCE AND
BIOTECHNOLOGY
DEPARTMENT OF AGRICULTURE, FORESTRY
AND BIORESOURCES
THE GRADUATE SCHOOL
OF SEOUL NATIONAL UNIVERSITY

Effect of Growth Progress on Positional Distribution of UV-B Light Interception and Bioactive Compound Contents in Kale

UNDER THE DIRECTION OF DR. JUNG EEK SON
SUBMITTED TO THE FACULTY OF THE GRADUATE SCHOOL OF
SEOUL NATIONAL UNIVERSITY

BY

HYUN YOUNG KIM

MAJOR IN HORTICULTURAL SCIENCE AND BIOTECHNOLOGY

DEPARTMENT OF AGRICULTURE, FORESTRY

AND BIORESOURCES

THE GRADUATE SCHOOL OF SEOUL NATIONAL UNIVERSITY
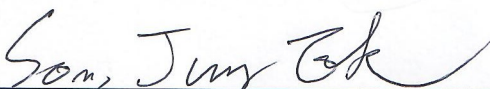
FEBRUARY, 2021

APPROVED AS A QUALIFIED THSIS OF HYUN YOUNG KIM

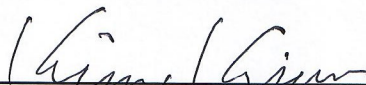FOR THE DEGREE OF MASTER OF SCIENCE

BY THE COMMITTEE MEMBERS

CHAIRMAN: _____
EUN JIN LEE, PH.D.

VICE-CHAIRMAN: _____
JUNG EEK SON, PH.D.

MEMBER: _____
KI SUN KIM, PH.D.

Effect of Growth Progress on Positional Distribution of UV-B Light Interception and Bioactive Compound Contents in Kale

Hyun Young Kim

Department of Agriculture, Forestry and Bioresources,

The Graduate School of Seoul National University

ABSTRACT

UV-B (280–315 nm) radiation has been used as an effective tool to improve bioactive compound contents in controlled environments, such as plant factories. However, plant structure changes with growth progress induce different positional distributions of UV-B radiation interception, which cause difficulty in accurately evaluating the effects of UV-B on biosynthesis of bioactive compounds. The objective of this study was to quantitatively analyze the positional distributions of UV-B radiation interception and bioactive compound contents of kales (*Brassica oleracea* L. var. *acephala*) with growth progress and their relationships. Plants were grown in a plant factory at a photosynthetic photon flux density of 200 μmol m^{-2} s^{-1} with a photoperiod of 16 h and were harvested at 14 and 28 days after transplanting (DATs). The plants were exposed to two different doses of UV-B radiation (e.g., 1.3 W m^{-2}

for 6 h or 12 h per day) for 1, 2, and 3 days before harvest. UV-B light interception, total phenolic compound (TPC), and total flavonoid compound (TFC) at the upper, middle and lower leaves of the plants were evaluated. Spatial UV-B radiation interception was analyzed by using 3D plant models and ray-tracing simulations. UV-B levels did not affect plant growth, including leaf area, fresh leaf weight, or dry weight. As growth progressed, the UV-B radiation interception amounts in the upper leaves were 34.1% and 88.8% higher than those for the middle and lower leaves, respectively. The bioactive compound contents in the upper leaves were 29.3–36.8% and 70.1–82.6% higher than those in the middle and lower leaves, respectively. The increase rates of TFC relative to the cumulative absorbed UV amounts were highest for the upper leaves of the 28 DAT plants, while those for TPC were highest in the middle leaves of the 14 DAT plants. Despite the same UV-B levels, the UV-B radiation interception and UV-B susceptibility in the plants varied with leaf position and growth stage, which induced the different biosynthesis of TFC and TPC. This attempt to interpret UV-B radiation interception will contribute to estimating and quantifying the production of bioactive compounds.

Additional key words: leaf position, phenolic content, plant structure, 3D analysis, UV yield, vertical farm

CONTENTS

LIST OF TABLES

LIST OF FIGURES

INTRODUCTION

Brassica vegetable crops are known to have beneficial effects on human health (Podsędek., 2007; Heimler et al., 2007; Francisco et al., 2017). Among them, kale (*Brassica oleracea* L. var. *acephala*), which is a rich source of health-promoting phytochemicals, such as polyphenols and carotenoids (Olsen et al., 2009; Walsh et al., 2015), has been widely cultivated and consumed for several centuries (Šamec et al., 2019). Recently, to improve individual phytochemicals, the nutritional contents and profiles of *Brassica* vegetables have been studied (Krumbein et al., 2010; Ishida et al., 2014). As strategies for optimizing and balancing these profiles, manipulation of environmental factors has been attempted (Oh et al., 2009; Davies and Espley, 2013). Variations in the amounts and patterns of compounds have been attributed to abiotic stress factors, including temperature, drought, salinity and ultraviolet (UV) radiation (Ramakrishna and Ravishankar, 2011; Linić et al., 2019; Podda et al., 2019; Toscano et al., 2019). In particular, UV-B (280–315 nm) has a great impact on plant defense mechanisms and is used as an effective tool to increase bioactive compound contents over short-term periods in various crops (Czégény et al., 2016; Escobar-Bravo et al., 2017; Yavaş et al., 2020).

Many previous studies have focused on the effects of UV-B energy (dosage) levels on bioactive compounds in many crops for application in controlled environments, such as plant factories (Martínez-lüscher et al., 2013;

Hectors et al., 2014; Zhao et al., 2020). UV-B levels have been determined from the energy emitted by UV-B light sources (Bian et al., 2014; Acharya et al., 2016). However, plant responses to UV-B are driven not by the energy released but by the energy absorbed by leaves (Meyer et al., 2009), which changes with leaf position (Morales et al., 2011). UV-B exposure on upper leaves was more advantageous for absorbing light, but lower leaves had no choice but to receive the transmitted light in the plant canopy (Filella and Peñuelas, 1999). In *Arabidopsis*, the light capture efficiency of simulated leaves with spiral phyllotaxis increased with leaf order (Strauss et al., 2020). Therefore, the accumulation pattern of UV-B absorbing compounds should be considered with respect to leaf position (Grammatikopoulos et al., 1999; Liakoura et al., 2003).

In most previous studies, accumulation of bioactive compounds according to leaf position has been interpreted as an influence of UV-B susceptibility that is related to leaf age (Behn et al., 2011; Majer and Hideg, 2012; Holub et al., 2019). Considering the three-dimensional (3D) plant structure, bioactive compounds at each leaf were determined with UV-B radiation interception as well as with leaf age in kale (Yoon et al., unpublished). As plant growth progresses, changes in lighting distance (Kim et al., 2020b) or planting density (Portes and Melo, 2014; Xue et al., 2015) can affect the spatial distribution of light interception for whole plants, which is directly related to plant growth and biomass production. Accumulation of bioactive compounds is regulated by the overall developmental stages of whole plants as well as by the specific

developmental state of each leaf (Lois, 1994). In particular, under UV-B exposure, secondary metabolites are affected by plant developmental ages in pak choi (Heinze et al., 2018). Therefore, plant growth progress may cause large variations in absorbed UV-B based on leaf position as well as the UV sensitivity due to leaf age. Their influences on metabolite accumulation cannot be distinguished without quantification of the absorbed UV-B energy distribution.

Recently, the light distribution for a whole plant was quantitatively analyzed using 3D plant models and ray-tracing simulation analysis (Kim et al., 2020a, Kim et al., 2020b). However, spatial analysis of light distribution has not been applied to UV-B radiation. These methods allow interpretations of absorbed UV-B distributions based on plant structure. This study hypothesized that, for individual plants, light interception depends on leaf position as well as growth stage, which will affect UV-B-induced biosynthesis of bioactive compounds. The objective of this study was to quantitatively analyze the positional distributions of UV-B radiation interception and bioactive compound contents of kales with growth progress and their relationships using 3D analysis.

LITERATURE REVIEW

UV-B Radiation to plants

Global concerns about depletion of stratospheric ozone have led to research about the effect of exposure to ultraviolet (UV) radiation on plants (McKenzie et al., 1999). Due to highly energetic shorter wavelength, UV-B (280–315 nm) induces a number of deleterious effects in plants (Caldwell et al., 1998), including inhibition of protein synthesis or photosynthesis reaction and cause damage of DNA, proteins, membrane lipids and even necrosis of plant cells (Brosché and Strid, 2003; Frohnmeyer and Staiger, 2003). Plants have specific UV-B photoreceptor, UV RESISTANCE LOCUS (UVR8), stimulates gene expression involved in nonspecific pathway as antioxidative defense and specific pathway to protect leaves from UV-B penetration (Jenkins, 2009; Parihar et al., 2015). Recent studies have highlighted the regulatory properties of low UV-B levels that allow plants to balance nonspecific and UV-B specific pathways and to avoid the side effects caused by UV-B exposure (Hideg et al., 2013; Czégény et al., 2016; Neugart and Schreiner, 2018). To find out moderate UV-B energy that trigger plant's secondary metabolism, various dosages consisting of exposure hour, duration, and recovery time have been applied in controlled environment (Brechner et al., 2011; Moreira-Rodríguez et al., 2017; Höll et al., 2019; Mosadegh et al., 2019).

Estimation of Secondary Metabolites in Plant Factory

Plant factory can control the growth conditions including abiotic stresses to accumulate bioactive compounds. The practical use of plant factory has been delayed due to high initial investment and electric power consumption, which cause low economic efficiency (Kozai, 2013). Therefore, plant factory should produce high-value added and high-quality crops which contain secondary metabolites as a way to enhance revenues (Lee et al., 2013). Since plant factory can facilitate planned and stable supply, the productivity of secondary metabolites could be estimated through modelling. The optimal harvest time for annual production of secondary metabolites in kale based on the continuous phase was determined to be 42 days after transplanting (Yoon et al., 2019). However, the annual production of secondary metabolites was simply estimated by few elements without effects of light environment or plant developmental age which is important factors of metabolites production. The effect of external factors or internal factors, and their interaction on secondary metabolites accumulation was quantified in few reports. In St. John's wort, light intensity, temperature, and growth stage affected the secondary metabolites accumulation individually but not at the same time (Radušienė et al., 2013). Also, the UV treatment, leaf age, and interaction between them individually affected the accumulation of flavonoid in two *Brassica* cultivars (Reifenrath and Müller, 2007).

Effect of Leaf Position and Growth Stage on Secondary Metabolites

Secondary metabolite accumulation in different leaf positions has been considered only as the influence of leaf age which is an important determinant of stress susceptibility (Behn et al., 2011; Majer and Hideg, 2012; Holub et al., 2019). For example, acclimation of young leaves to water stress involved higher homeostasis of ROS and metabolites than mature leaves in *Arabidopsis* (Sperdouli and Moustakas, 2014). Furthermore, leaf's physiological age at the time of leaf formation from the primordial tissue affected the essential oil composition in sweet basil because of trichome density and enzyme activity (Deschamps and Simon, 2010; Fischer et al., 2011). However, leaf positions in individual plant contain both physiological and structural characteristics. The spatial and temporal effect of herbicide stress on different leaf position considering plant structure was monitored using chlorophyll fluorescence imaging (Konishi et al., 2009). Also, the leaf position with more UV-B exposure appeared lower F_v/F_m value, and higher concentration in bioactive compounds in kale (Yoon et al., 2020). Meanwhile, Heinze et al. (2018) reported that the change in secondary metabolite profiles are greatly affected by developmental stage which is linked to increase in fresh weights and leaf areas.

MATERIALS & METHODS

Plant Materials and Growth Conditions

Kale seeds (*Brassica oleracea* L. var. *acephala*, 'Manchoo collard,' Asia Seed Company, Seoul, Korea) were sown and germinated on sponge cubes by hydroponic methods under fluorescent lamps at a photosynthetic photon flux density (PPFD) of 150 μmol m^{-2} s^{-1}. After the first leaf appeared, the nutrient solution for *Brassica* (Choi et al., 2005) was applied, which had an electrical conductivity (EC) of 0.6 dS m^{-1}. At four weeks after germination, seedlings were transplanted into plant factory modules with a deep flow technique system, and each module was 150 H × 80 W × 50 L (cm) in size. The modules were maintained at 24°℃/20℃ light/dark temperatures, 70% relative humidity, and 500 μmol mol^{-1} CO_2 concentration. The transplanted plants were irradiated with light-emitting diodes (LEDs) at 200 μmol m^{-2} s^{-1} over a waveband of 400–700 nm for a 16 h light period and were supplied with 1.2 dS m^{-1} EC nutrient solution. Three plants per treatment were harvested at 14 days after transplanting (DAT), and two plants per treatment were harvested at 28 DAT.

Growth Characteristics

Fresh leaf weights were determined at harvest with three replicates, and dry leaf weights were measured after drying in an oven for 120 or 168 h for the 14 DAT and 28 DAT plants, respectively. After photographing all leaves, total

plant leaf areas were calculated with the image analysis software ImageJ (National Institutes of Health, Bethesda, MD, USA).

UV-B Treatment

All plants were irradiated with supplemental UV-B LEDs (Ericsong Company Ltd., Bucheon, Korea) with 1.2 W m^{-2} at a spectrum peak approximately 310 nm. UV-B exposure periods were 6 and 12 h per day for 1, 2, and 3 days before harvest, which resulted in a total of six treatments (e.g., 1 d 6 h, 1 d 12 h, 2 d 6 h, 2 d 12 h, 3 d 6 h and 3 d 12 h), which were equivalent to cumulative UV-B doses of 21.6, 43.2, 43.2, 86.4, 64.8, and 129.6 kJ m^{-2} d^{-1}, respectively. After UV-B exposure, all plants had a recovery time of 4 h per day, and plants from all treatments were harvested simultaneously. The experimental setup is shown in Fig. 1. UV-B irradiation was measured by a UV sensor (MU-200, Apogee Instruments Inc., Logan, UT, USA) and spectroradiometer (Blue-Wave spectrometer, StellarNet Inc., Tampa, FL, USA).
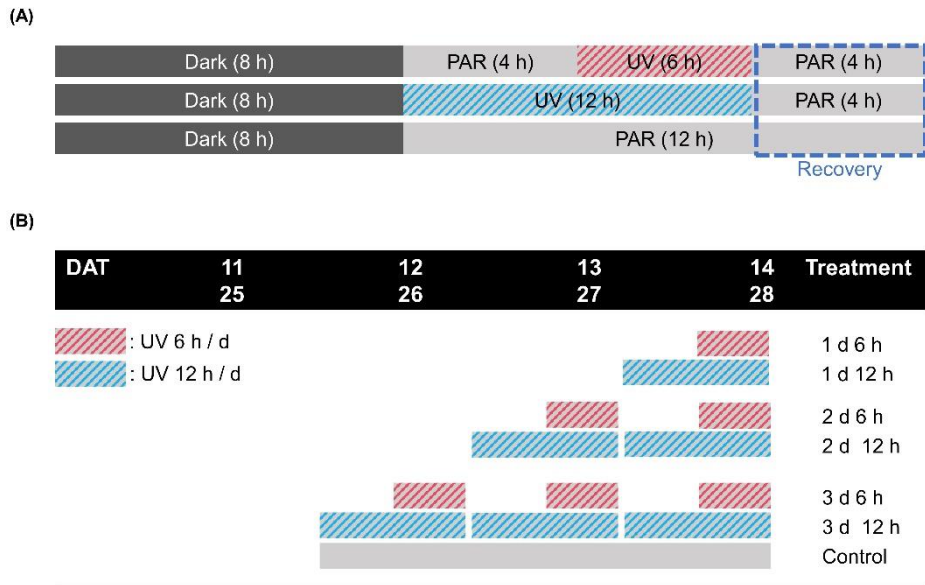
Fig. 1 Experimental design. Daily UV-B exposures and recovery times are shown at the top (A). The schedules of UV-B treatments and each measurement (B) were the same for both harvest dates at 14 and 28 days after transplanting (DATs).

Chlorophyll Fluorescence

Chlorophyll fluorescence was measured for 30-min dark-adapted leaves using a chlorophyll fluorescence meter (Handy PEA fluorometer, Hansatech, Kings Lynn, UK) according to a previous study (Rapacz, 2007). At 14 and 28 DATs, all measurements were performed after the recovery time with three replicates. Measurements were performed using a saturating pulse of 1,500 µmol m^{-2} s^{-1} for 1 s to determine the minimal fluorescence (F_0) and maximal fluorescence (F_m) values. The maximal photochemical efficiency of photosystem II (F_v/F_m) was calculated as $(F_m - F_0)/F_m$.

Bioactive Compounds and Antioxidant Capacity

Total Phenolics

Total phenolic compounds (TPCs) were measured by the Folin-Ciocalteu colorimetric method (Ainsworth and Gillespie, 2007). Powdered samples (500 mg) were mixed with 1 mL of 80% methanol, incubated for 48 h in the dark at room temperature and centrifuged at 5,500 × g for 10 min. Supernatants of samples (50 µL) were collected in 2 mL microtubes and were then mixed with 750 µL of 10% Folin–Ciocalteu solution and 135 µL of distilled water using a vortexer. After mixing, 600 µL of 700 mM Na_2CO_3 was added, and the samples were then incubated for 2 h at room temperature. Sample absorbances were read at 765 nm using a spectrophotometer (Photolab 6100vis, Weilheim, Germany).

The standard unit for TPC was expressed as milligrams of gallic acid equivalent per gram of dry weight (mg GAE g^{-1} DW).

Total Flavonoids

Total flavonoid compound (TFC) amounts were measured by an aluminum chloride colorimetric method (Dewanto et al., 2002; Lee et al., 2012). Powdered samples (500 mg) were mixed with 1 mL of 80% methanol, incubated for 12 h in the dark at 4°C, and centrifuged at 1.1×104 g for 10 min. The supernatants (50 μL) of the samples were collected in 2 mL microtubes, and 135 μL of distilled water and 45 μL of 5% $NaNO_2$ were added. Ninety microliters of 10% $AlCl_3$ and 300 μL of 1 M NaOH were added after 5 and 6 min, respectively, and 165 μL of distilled water was then added. After incubating for 30 min, sample absorbances were then read at 510 nm using a spectrophotometer, and the standard unit for TFC was expressed as milligrams of catechin acid equivalent per gram of dry weight (mg CE g^{-1} DW).

Antioxidant Capacity

Total antioxidant capacity was measured using the 2,2-diphenyl-1-picrylhydrazyl (DPPH) assay method (Brand-Williams et al., 1995; Andarwulan et al., 2010). A DPPH solution was prepared with 500 mL of 80% methanol and 12 mg of DPPH. Samples were incubated for 48 h in the dark at

room temperature and were centrifuged at $11,000 \times g$ for 10 min. Supernatants (50 μL) were then collected in 2 mL microtubes, and 1.95 mL of DPPH solution was added. After incubating for 30 min, the sample absorbances were then read at 517 nm by the spectrophotometer and used methanol as the blank. Antioxidant activity was expressed as radical scavenging activity (*RSA*), which was calculated using the following equation:

$$RSA\,(\%) = (A_{control\ 517nm} - A_{sample\ 517nm})\,/\,A_{control\ 517nm}\ \times\ 100 \quad (1)$$

where the $A_{control\ 517nm}$ and $A_{sample\ 517nm}$ are the absorbances of the samples at 517nm without and with leaf extract, respectively.

Construction of 3D-scanned Plant Models

The plants used to reconstruct 3D-scanned plant models were scanned with a high-resolution portable 3D scanner (GO!SCAN50TM, CREAFORM, Lévis, Quebec, Canada). The scanner resolution was set at 2 mm. Plants representing 3 d 6 h, 3 d 12 h, and the control were scanned before and after treatments. The scanned data were obtained with Vxelement scanning software (CREAFORM, Lévis). Holes and noise in the 3D mesh data were fixed, and segmented mesh data were reconstructed to a surface model to perform ray-tracing simulations

by reverse engineering software (Geomagic Design X, 3D Syst6ems, Rock Hill, SC, USA).

Ray-tracing Simulation

For the ray tracing simulations, the transmittance and reflectance of each leaf position and module material were measured with a spectroradiometer in a range of 250–700 nm to determine optical properties for the plant models. A virtual growth bed and LED bars were reconstructed using 3D computer-aided design software (Solidworks, Dassault Systèmes, Vélizy-Villacoublay, France). Ray-tracing simulations were performed by using a ray-tracing software (Optisworks, OPTIS Inc., La Farlède, France). Simulation outputs for six plant models per treatment were averaged. By setting the value for each leaf as a detector, the average light interceptions in the range of photosynthetically active radiation (PAR) at 400–700 nm and UV at 250–400 nm were obtained.

Statistical Analysis

One-way and two-way analysis of variance (ANOVA) and Tukey's HSD test were used to compare the means among treatments with R software (R 1.2.5, R Foundation, Vienna, Austria). The UV energy yields for TPC and TFC contents were obtained with nonlinear regression as

$$\Delta C = a/\Delta UV + b \tag{2}$$

where a and b are the regression coefficients for the relationships between bioactive compounds and absorbed UV, respectively. ΔC is the increase rate of TPC and TFC contents compared to the control, and ΔUV is the UV absorbed on leaves in each treatment. Linear and nonlinear regressions were conducted with Python (Python 3.6.7, Python Software Foundation, Wilmington, USA).

RESULTS

Plant Growth

The plant growth characteristics did not show any significant differences among the treatments at either growth stage during cultivation (Fig. 2). In the $UV_{12 h}$ treatments (e.g., 1 d 12 h, 2 d 12 h, and 3 d 12 h), fresh leaf weights and dry leaf weights slightly decreased with the UV-B exposure period at 28 DAT (Figs. 2C–F), and leaf areas were 10–25% lower than those of the control (Figs. 2A, B). F_v/F_m values at 14 and 28 DATs were 0.82–83 in all treatments and did not differ among treatments (data not shown). Therefore, UV-B levels did not affect the growth or photochemical efficiency in all treatments.
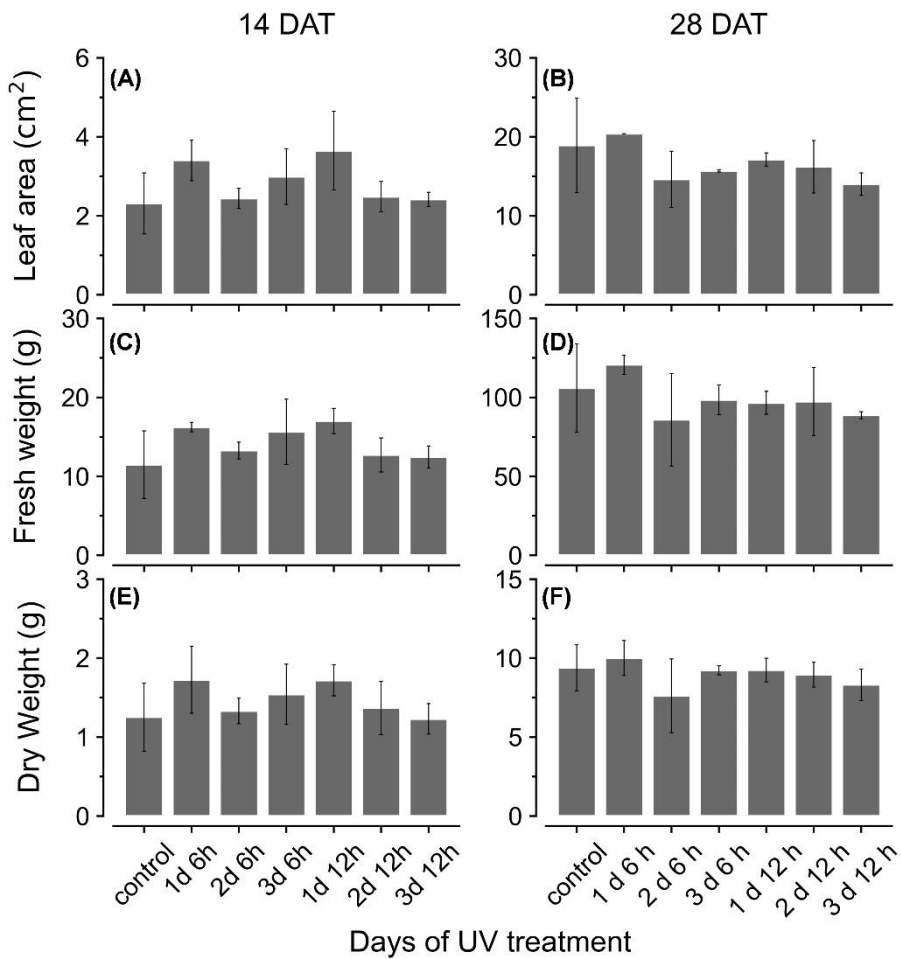
Fig. 2 Leaf areas (LA; A, B); fresh leaf weights (FW; C, D); and dry weights (DW; E, F) of kales at 14 and 28 days after transplanting (DATs) as affected by UV-B exposure periods of 6 h and 12 h per day.

Vertical Distributions of PAR and UV Radiation Interception

PAR and UV radiation interceptions were simulated well with the 3D structure of the plants, i.e., leaf positions and leaf angles (Fig. 3). Radiation interception levels increased with plant height and leaf position in the order of upper, middle and lower leaves for both growth stages (Fig. 4). Plants at 14 DAT had lower plant heights but the leaves at each position received higher light intensities compared to those at 28 DAT (Fig. 4A). At 14 DAT, the absorbed UV levels of the upper leaves were 12.1% and 54.5% higher than those of the middle and lower leaves, respectively (Fig. 4B). The differences in absorbed UV light between leaf positions were more pronounced at 28 DAT, for which the UV radiation interceptions of the upper leaves were 34.1% and 88.8% higher than those of the upper leaves, respectively.
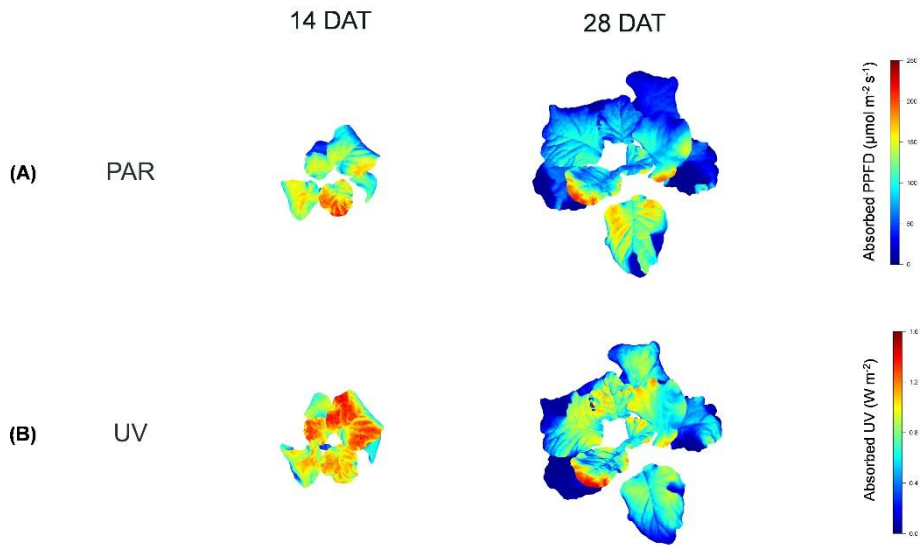
Fig. 3 Light interception distributions of PAR of 400-700 nm (A) and UV of 250-400 nm (B) on 3D-scanned kale models under PAR or UV-B LEDs at 14 and 28 days after transplanting (DATs).
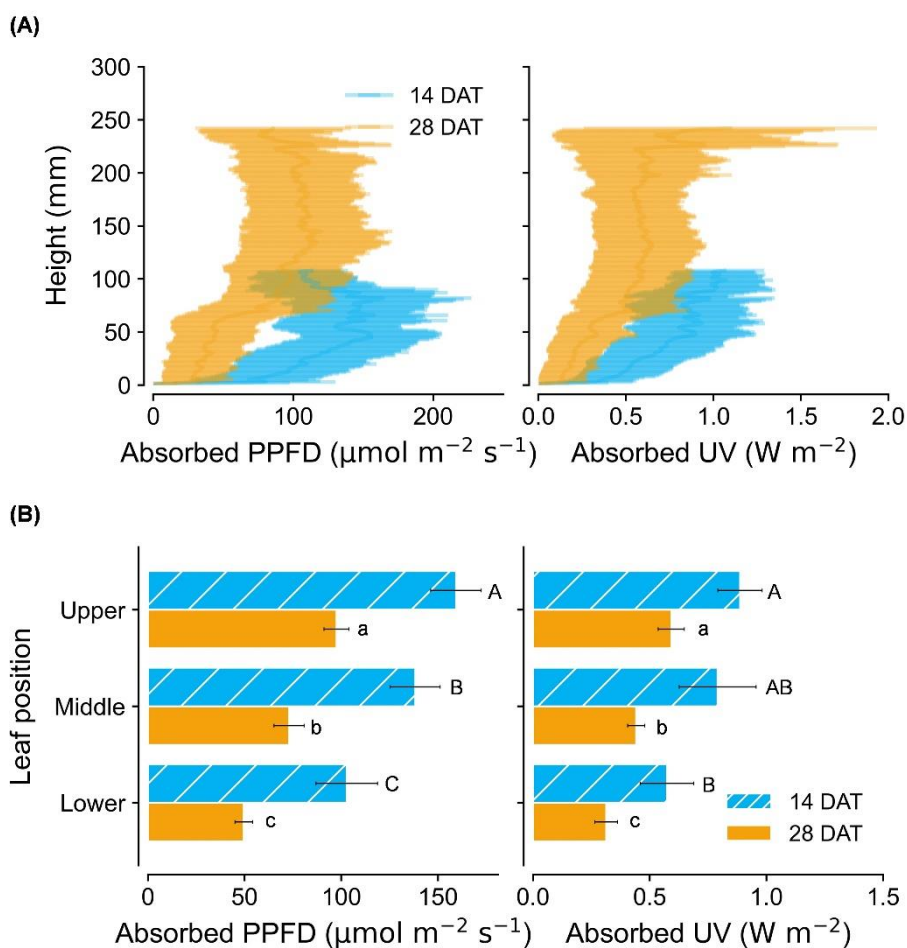
Fig. 4 Vertical distributions of photosynthetic photon flux density (PPFD) and UV radiation (250–400 nm) interception of kales according to plant heights (A) and leaf positions (B) at 14 and 28 days after transplanting (DATs). Different letters represent significant differences ($p \leq 0.005$ by two-way ANOVA and Tukey's HSD test) for leaf positions of the 14 and 28 DAT plants.

19

Bioactive Compounds and Antioxidant Capacity

TFC and TPC concentrations and antioxidant capacity (RSA) were higher with greater UV-B exposure and higher leaf positions (Fig. 5). Only on the upper leaves at 14 DAT were the TFC and TPC levels significantly higher than those at other positions (Figs. 5A, C, E), while those at 28 DAT increased significantly in the order of upper, middle, and lower leaves (Figs. 5B, D, F). In all treatments at 14 DAT, the TFC and TPC levels in the upper leaves were 35.9–63.1% and 29.6–55.2% higher than those of the other leaves, respectively. At 28 DAT, those values in the upper leaves were 29.3–36.8% and 70.1–82.6% higher than those of the other leaves, respectively. Overall, the TFC, TPC and RSA values for the 2 d 12 h and 3 d 12 h treatments were higher than those for the control at both growth stages.
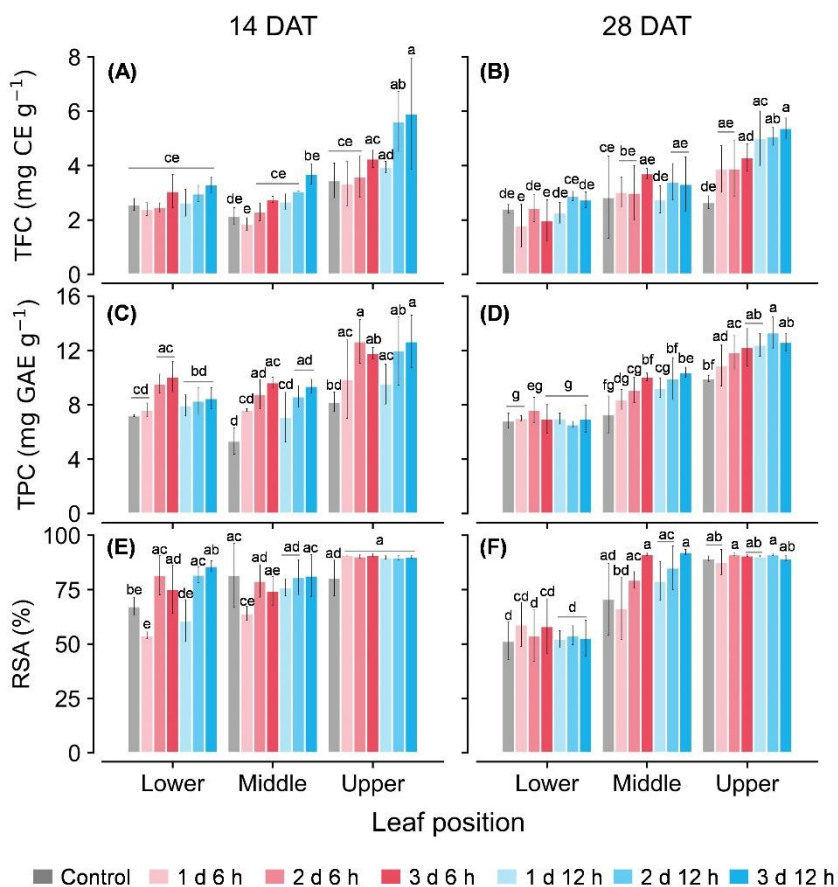
Fig. 5 Concentrations of total flavonoid compounds (TFC; A, B); total phenolic compounds (TPC; C, D); and radical scavenging activities (RSA; E, F) of kales grown under control and UV-B treatments according to leaf positions and growth stages (days after transplanting, DAT). Different letters represent significant differences ($p \leq 0.005$ by two-way ANOVA and Tukey's HSD test) for TFC, TPC and RSA.

Relationships Between UV Radiation Interception and Bioactive Compounds

Across all data, the TPC and TFC concentrations relative to the cumulative amounts of UV absorbed for 3 days showed linear relationships at each leaf position (Fig. 6). The coefficients of determination (R^2) of the linear regressions are shown in Table 1. As growth progressed from 14 to 28 DATs, the gradients of TFC levels against absorbed UV increased slightly for the upper leaves (Figs. 6A, B). In contrast, the gradients of TPC levels for the upper leaves decreased by 25% but only increased by 13.8% in the middle leaves at 28 DAT compared to those at 14 DAT.

Changes in TFC and TPC levels relative to cumulative absorbed UV amounts were regressed according to leaf positions and growth stages using rectangular hyperbolic equations (Fig. 7, Eq. 2). The R^2 values of these nonlinear regressions are shown in Table 1. The patterns of increase rates, i.e., the cumulative UV energy yields were dependent on the type of bioactive compound. UV yields for TFC were highest in the upper leaves at 28 DAT (Fig. 7B), but those among leaf positions did not differ noticeably at 14 DAT (Fig. 7A). On the other hand, UV yields for TPC were highest in the middle leaves at both growth stages and decreased for all leaf positions at 28 DAT compared to those at 14 DAT (Fig. 7C, D).
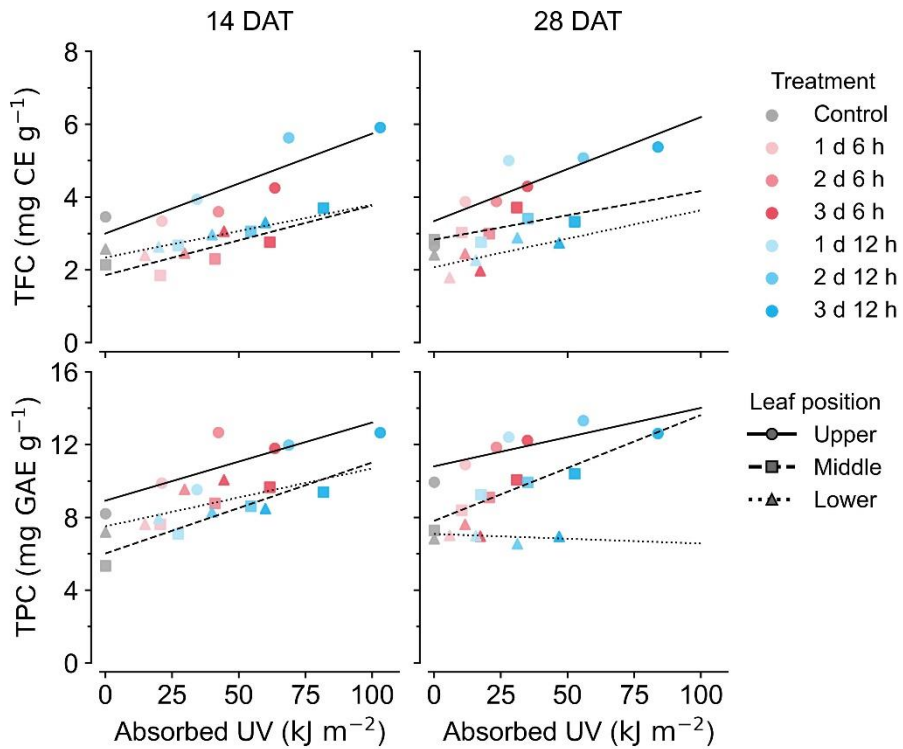
Fig. 6 Relationships between total flavonoid compounds (TFC; A, B); total phenolic compounds (TPC; C, D); and cumulative absorbed UV for 3 days of kales grown under the control and UV-B treatments according to leaf positions and growth stages (days after transplanting, DAT).

Table 1 Coefficients of determination (R^2) from linear regressions for bioactive compound contents and from nonlinear regressions for change rates with cumulative absorbed UV for 3 days according to leaf position and growth stage. Refer to Eq. 2 for the nonlinear regression equation.

Growth stage	Leaf position	Linear regression		Nonlinear regression	
		TFC[z]	TPC[y]	TFC	TPC
14 DAT[x]	Upper	0.79	0.70	0.64	0.59
	Middle	0.73	0.84	0.66	0.74
	Lower	0.73	0.39	0.71	0.37
28 DAT	Upper	0.73	0.64	0.59	0.84
	Middle	0.45	0.87	0.34	0.91
	Lower	0.41	0.07	0.61	0.11

[z]TFC, total flavonoid compounds

[y]TPC, total phenolic compounds

[x]DAT, days after transplanting
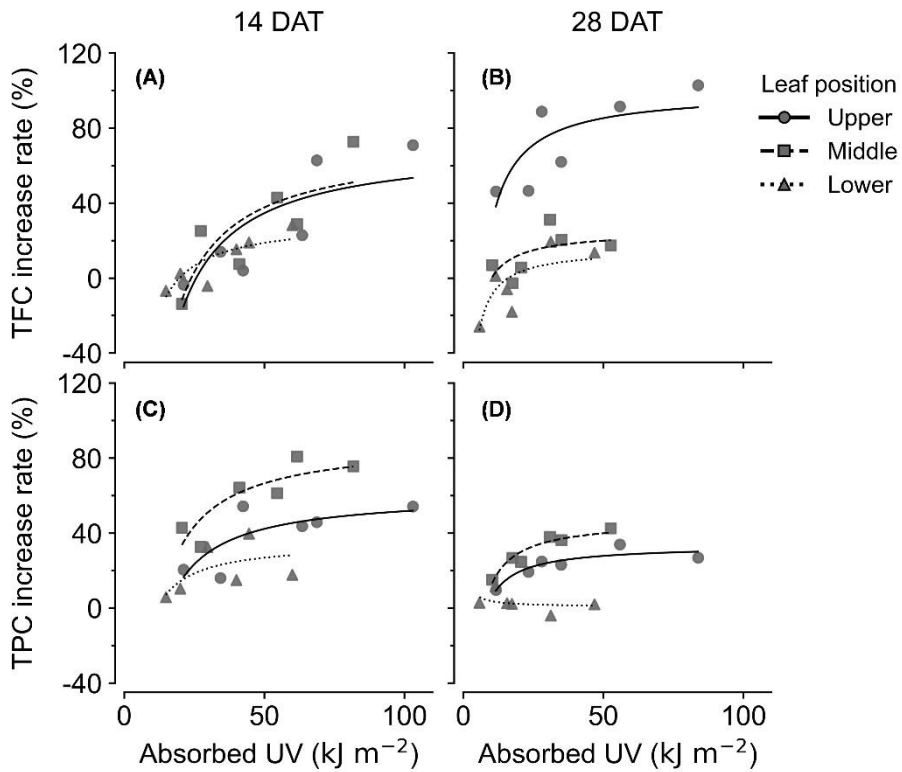
Fig. 7 Increase rates of total flavonoid compounds (TFC; A, B) and total phenolic compounds (TPC; C, D) relative to cumulative absorbed UV of kales according to leaf positions and growth stages (days after transplanting, DAT).

DISCUSSION

Effect UV-B Radiation on Plant Growth

In most previous studies, growth inhibition in UV-B-acclimated plants was observed for numerous species (Hofmann et al., 2001; Jansen, 2002; Hectors et al., 2007). As growth progressed, all growth characteristics under UV-B exposure were slightly lower than those of the control (Fig. 2). In addition, F_v/F_m values for all treatments remained at 0.82–83, which indicated normal growth conditions (Baker, 2008). Therefore, the UV-B levels used in this study were not high enough to affect growth or photosystem II activity.

UV-B Radiation Interception with Growth Progress

Several studies have determined the spatial distributions of light interception in plant canopies by use of a mathematical or functional structural plant model in soybean, maize, and tomato (Yang et al., 1993; Stewart et al., 2003; Sarlikioti et al., 2011). Similar to previous results, UV radiation interception increased with leaf height and leaf position for both growth stages (Figs. 3 and 4). However, average light interception decreased with growth progress for all leaf positions (Fig. 4B). In contrast, previous reports for taller crops showed higher light interception than for shorter crops with growth progress (Xue et al., 2015; Cabrera-Bosquet et al., 2016). Unlike natural light, the narrow radiation range of artificial light sources, such as LEDs in controlled

environments, affects the irradiation area depending on planting conditions (Kim et al., 2020b). Although the higher and upper leaves were irradiated directly under the UV LED at 28 DAT, the average light interception would have been relatively low. As growth progresses, higher planting density causes shading at the single or canopy level and reduces UV-B radiation interception along with the narrow radiation range of LEDs. Kang et al. (2019) found in paprika that the estimated light interception rapidly decreased with a relatively higher planting density arrangement. Due to the higher planting density, leaf angles in the middle leaves were twisted close to 90° or overlapped with each other and thus prevented irradiation. Similar to *Arabidopsis*, which has spiral phyllotaxis leaves at intervals of 137.5°, kale's overlapping leaves within individual plants affect light interception patterns (Strauss et al., 2020). Therefore, these results showed that the positional distributions of light interception were altered by self-shading or by neighboring plants with growth progress.

Bioactive Compound Accumulation with Growth Progress

UV-B has been used to irradiate various crops to enhance bioactive compound contents in controlled environments (Czégény et al., 2016; Yavaş et al., 2020). In this study, the longer UV-B durations of both daily time and exposure days induced higher TFC and TPC levels (Fig. 5). Similarly, a UV-B

dose-dependent response of biosynthesized secondary metabolites was found in St. John's wort and sweet basil, which were exposed to repeated doses for a few days (Brechner et al., 2011; Mosadegh et al., 2018). However, the UV-dose dependence of TFC and TPC at 28 DAT appeared only in the upper leaves, which were exposed to higher UV-B intensities (Figs. 4 and 5). As growth progressed, similar to the vertical distribution of light interception, the differences in UV-B-induced TFC and TPC among leaf positions became highly distinct (Fig. 5). This result suggested that the patterns of bioactive compound accumulation were affected by UV radiation interception patterns according to plant structure. A previous study indicated that flavonol profiles were highly associated with characteristics that were related to canopy structure and light interception (Martínez-Lüscher et al., 2019). One of the main flavonoids, catechins, in an albino tea cultivar, significantly decreased with plant shading, which was associated with DNA methylation involved in the flavonoid biosynthesis pathway (Xu et al., 2020). In this study, RSA levels in the upper leaves were also highest for both growth stages (Figs. 5E, F). Antioxidant capacity is an indicator that can indirectly show a plant's physiological ability of its leaves (Blum-Silva et al., 2015). Phenolic acids and flavonoids containing catechol structures have been highly correlated with their radical scavenging capacity (Ayaz et al., 2008; Zietz et al., 2010; Fiol et al., 2012).

On the other hand, the growth progress caused large variations in leaf age within plants. Heinze et al. (2018) reported that phenolic and hydroxycinnamic acids accumulated to higher levels in plants with mature leaves than in plants with younger leaves, which indicated that they can also be applied to mature and young leaves in individual plants. In this study, TFC and TPC levels in lower (older) leaves at 28 DAT showed the lowest values among treatments (Figs. 5C, D). RSA levels in lower leaves at 28 DAT were significantly lower than those at 14 DAT (Figs. 5E, F). Even for the same position, the leaf ages of the lower leaves were at least 2 weeks at 14 DAT and were at least 4 weeks at 28 DAT. Similarly, younger leaves also exhibited higher antioxidant capacities than older leaves in grapevines (Majer and Hideg, 2012).

Cumulative UV Energy Yield for Accumulation of Bioactive Compounds

The linear correlations between TPC and TFC levels and cumulative UV absorbed for 3 days were clearly distinguished by leaf position (Fig. 6). The gradient of the regression line presented in a previous report has been interpreted as the radiation use efficiency under PAR light (Chakwizira et al., 2014). In this study, the gradient of the regression line was interpreted as the UV-B stress susceptibility of leaves, which is involved with leaf age. As growth progressed, the TFC increase rate in the upper leaves increased noticeably, which indicated that the upper leaves were greatly affected by UV-B radiation

interception (Fig. 7B). In other words, young leaves had the highest UV-B susceptibility for TFC (Fig. 7), which was consistent with previous findings of general stress susceptibility with leaf age (Sperdouli and Moustakas, 2014b; Moustaka et al., 2015; Kanojia et al., 2020). Canopy distributions of nitrogen (N) and phosphorus, whose levels remained constant or gradually decreased in aging leaves, were inferred to be related to UV energy yields for TFC and TPC (Coleman, 1986; Chakwizira et al,. 2011). Radiation use efficiency was determined not only by canopy N distributions but also by leaf N allocations in the thylakoid light-harvesting proteins of *Brassica* crops (Fletcher et al., 2013; Liu et al., 2020). However, although the actual leaf ages of the upper leaves were the same at approximately 1–2 weeks from their appearance between 14 and 28 DATs, the TFC increase rate was markedly higher at 28 DAT (Figs. 7A, B). In other words, cumulative UV energy yields for TFC were determined by plant developmental ages as well as by leaf ages. In contrast with the TFC results, the UV-B increase rate for TPC was highest in the middle leaves (Figs. 6 and 7). Similarly, previous studies showed that UV-B-induced metabolite accumulations depended on chemical structure as well as chalcone synthase activity (Neugart et al., 2012; Ghasemzadeh et al., 2016).

As growth progressed, the TFC and TPC increase rates increased or decreased for all leaf positions, which indicated changes in UV-B susceptibility (Fig. 7), but the actual concentrations were similar between 14 and 28 DATs (Figs. 5 and 7). These results were caused by both higher UV-B light

interception at 14 DAT and higher concentrations with growth progress in the control without UV-B exposure. This tendency is consistent with the results of a previous study, which showed increases in bioactive compounds and total glucosinolate contents in kale without UV-B exposure in plant factories (Yoon et al., 2019).

Despite the predominance of UV-B susceptibility in the middle leaves at 28 DAT (Fig. 7D), actual TPC concentrations were significantly higher in the upper leaves (Fig. 5D). If the amount of UV radiation interception in the middle leaves was not intercepted by the upper leaves at 28 DAT, TPC concentrations in the middle leaves could be higher than those in the upper leaves. Therefore, the UV-B-induced bioactive compound contents in the plant structure were determined by the age-dependent cumulative UV energy yields as well as by distributions of UV-B radiation interception.

Application to Bioactive Compounds Production in Plant Factories

This study confirmed that the absorbed UV-B and bioactive compounds at three leaf positions were affected by plant structure and growth stage, and that the growth progress induced changes in age-dependent UV-B energy yields for TFC and TPC as well as plant structure. Unexpectedly, the UV susceptibility of TPC was highest in the middle leaves for both growth stages. Considering the largest proportion of the middle leaves in plants, further studies need to

investigate the lateral UV-B irradiation method that focuses on the middle leaves. In addition, it is important to determine the growth stage when the upper leaves entirely cover the middle leaves so that the independent effect of UV radiation interception by the middle or lower leaves can be completely confirmed. Several studies of light interception using 3D plant models and ray-tracing simulation analysis have been applied only to PAR light (Vos et al., 2010). This study successfully expanded the range of light interception to UV-B and showed its applicability to other crops with self- or neighboring shading in controlled environments. In a previous study, the annual production of bioactive compounds in plant factories could be estimated using the content per plant at various growth stages without neighboring shading (Yoon et al., 2019). By applying this method, estimating the precise amounts of bioactive compounds with UV-B exposure can be performed under normal growth conditions with neighboring shading. Ultimately, it is possible to estimate bioactive compound production at the canopy level in controlled environments through UV-B radiation interception analysis.

CONCLUSION

The positional distributions of UV-B radiation interception and bioactive compound contents in kale leaves were quantitatively analyzed with 3D-scanned plant models and 3D light analysis. Concentrations of total flavonoid and phenolic compounds showed their highest values in the upper leaves for both growth stages. As growth progressed, variations in absorbed UV-B, as well as UV susceptibility, at each leaf position became evident. This study confirmed that biosynthesis of bioactive compounds in plant structures was determined by UV-B radiation interception and cumulative UV-B energy yield based on leaf position, leaf age, and plant growth stage. This attempt to quantitatively analyze the relationships between secondary metabolites and UV-B light interception can be applied to model bioactive compound production in plant factories.

LITERATURE CITED

Acharya J, Rechner O, Neugart S et al (2016) Effects of light-emitting diode treatments on *Brevicoryne brassicae* performance mediated by secondary metabolites in Brussels sprouts. J Plant Dis Prot 123:321–330.

Ainsworth EA, Gillespie KM (2007) Estimation of total phenolic content and other oxidation substrates in plant tissues using Folin-Ciocalteu reagent. Nat Protoc 2:875–877.

Andarwulan N, Batari R, Sandrasari DA et al (2010) Flavonoid content and antioxidant activity of vegetables from Indonesia. Food Chem 121:1231–1235.

Ayaz FA, Hayirlioglu-Ayaz S, Alpay-Karaoglu S et al (2008) Phenolic acid contents of kale (*Brassica oleraceae* L. var. *acephala* DC.) extracts and their antioxidant and antibacterial activities. Food Chem 107:19–25.

Baker NR (2008) Chlorophyll Fluorescence: A Probe of Photosynthesis In Vivo. Annu Rev Plant Biol 59:89–113.

Behn H, Schurr U, Ulbrich A, Noga G (2011) Development-dependent UV-B Responses in Red Oak Leaf Lettuce (Lactuca sativa L.): Physiological Mechanisms and Significance for Hardening. Eur J Hortic Sci 76:33–40.

Bian ZH, Yang C, Ke W (2014) Effects of light quality on the accumulation of phytochemicals in vegetables produced in controlled environments: A review. J Sci Food Agric 95:869–877.

Blum-Silva CH, Chaves VC, Schenkel EP et al (2015) The influence of leaf age on methylxanthines, total phenolic content, and free radical scavenging capacity of *Ilex paraguariensis* aqueous extracts. Rev Bras Farmacogn 25:1–6.

Brand-Williams W, Cuvelier ME, Berset C (1995) Use of a Free Radical Method to Evaluate Antioxidant Activity. LWT - Food Sci Technol 28:25–30.

Brechner ML, Albright LD, Weston LA (2011) Effects of UV-B on Secondary Metabolites of St. John's wort (*Hypericum perforatum* L.) grown in controlled environments. Photochem Photobiol 87:680–684.

Brosché M, Strid Å (2003) Molecular events following perception of ultraviolet-B radiation by plants. Physiol Plant 117:1–10.

Cabrera-Bosquet L, Fournier C, Brichet N et al (2016) High-throughput estimation of incident light, light interception and radiation-use efficiency of thousands of plants in a phenotyping platform. New Phytol 212:269–281.

Caldwell MM, Björn LO, Bornman JF et al (1998) Effects of increased solar ultraviolet radiation on terrestrial ecosystems. J Photochem Photobiol B Biol 46:40–52.

Chakwizira E, Brown HE, Ruiter JM De (2014) Radiation-use efficiency for forage kale crops grown under different nitrogen application rates. Grass Forage Sci 70:620–630.

Chakwizira E, Moot DJ, Scott WR et al (2011) Leaf development , radiation interception and radiation-use efficiency of kale crops supplied with different rates of banded or broadcast phosphorus fertiliser. Crop Pasture Sci 62:840.

Choi KY, SEO TC, Suh HD (2005) Development of nutrient solution for hydroponics of cruciferae leaf vegetables based on nutrient-water absorption rate and the cation ratio. Prot. Hortic. Plant Fact. 14:288–296

Coleman JS (1986) Leaf development and leaf stress : Increased susceptibility associated with sink-source transition. Tree Physiol 2:289–299.

Czégény G, Mátai A, Hideg É (2016) UV-B effects on leaves-Oxidative stress and acclimation in controlled environments. Plant Sci 248:57–63.

Davies K, Espley R (2013) Opportunities and challenges for metabolic engineering of secondary metabolite pathways for improved human health characters in fruit and vegetable crops. New Zeal J Crop Hortic Sci 41:154–177.

Deschamps C, Simon JE (2010) Phenylpropanoid biosynthesis in leaves and glandular trichomes of basil (*Ocimum basilicum* L.). Methods Mol Biol 643:263–273.

Dewanto V, Xianzhong W, Adom KK, Liu RH (2002) Thermal processing enhances the nutritional value of tomatoes by increasing total antioxidant activity. J Agric Food Chem 50:3010–3014.

Escobar-Bravo R, Klinkhamer PGL, Leiss KA (2017) Interactive effects of UV-B light with abiotic factors on plant growth and chemistry, and their consequences for defense against arthropod herbivores. Front Plant Sci 8:1–14.

Filella I, Peñuelas J (1999) Altitudinal differences in UV absorbance, UV reflectance and related morphological traits of *Quercus ilex* and *Rhododendron ferrugineum* in the mediterranean region. Plant Ecol 145:157–165.

Fiol M, Adermann S, Neugart S et al (2012) Highly glycosylated and acylated flavonols isolated from kale (*Brassica oleracea* var. *sabellica*) - Structure-antioxidant activity relationship. Food Res Int 47:80–89.

Fischer R, Nitzan N, Chaimovitsh D et al (2011) Variation in essential oil composition within individual leaves of sweet basil (*Ocimum basilicum* L .) is more affected by leaf position than by leaf age. J Agric Food Chem 59:4913–4922.

Fletcher AL, Johnstone PR, Chakwizira E, Brown HE (2013) Radiation capture and radiation use efficiency in response to N supply for crop species with contrasting canopies. F Crop Res 150:126–134.

Francisco M, Tortosa M, Martínez-Ballesta M de. C et al (2017) Nutritional and phytochemical value of *Brassica* crops from the agri-food perspective. Ann Appl Biol 170:273–285.

Frohnmeyer H, Staiger D (2003) Ultraviolet-B radiation-mediated responses in Plants. Balancing Damage and Protection. Plant Physiol 133:1420–1428.

Ghasemzadeh A, Ashkani S, Baghdadi A et al (2016) Improvement in flavonoids and phenolic acids production and pharmaceutical quality of sweet basil (*Ocimum basilicum* L.) by Ultraviolet-B irradiation. Molecules 21:1203.

Grammatikopoulos G, Petropoulou Y, Manetas Y (1999) Site-dependent differences in transmittance and UV-B-absorbing capacity of isolated leaf epidermes and mesophyll in *Urginea maritima* (L.) Baker. J Exp Bot 333:517–521.

Hectors K, Prinsen E, De Coen W et al (2007) *Arabidopsis thaliana* plants acclimated to low dose rates of ultraviolet B radiation show specific changes in morphology and gene expression in the absence of stress symptoms. New Phytol 175:255–270.

Hectors K, Van Oevelen S, Geuns J et al (2014) Dynamic changes in plant secondary metabolites during UV acclimation in *Arabidopsis thaliana*. Physiol Plant 152:219–230.

Heimler D, Isolani L, Vignolini P et al (2007) Polyphenol content and antioxidative activity in some species of freshly consumed salads. J Agric Food Chem 55:1724–1729.

Heinze M, Hanschen FS, Wiesner-Reinhold M et al (2018) Effects of developmental stages and reduced UVB and low UV conditions on plant

secondary metabolite profiles in pak choi (*Brassica rapa* subsp. *chinensis*). J Agric Food Chem 66:1678–1692.

Hideg É, Jansen MAK, Strid Å (2013) UV-B exposure, ROS, and stress: inseparable companions or loosely linked associates? Trends Plant Sci 18:107–115.

Hofmann RW, Campbell BD, Fountain DW et al (2001) Multivariate analysis of intraspecific responses to UV-B radiation in white clover (*Trifolium repens* L.). Plant, Cell Environ 24:917–927.

Höll J, Lindner S, Walter H et al (2019) Impact of pulsed UV-B stress exposure on plant performance: How recovery periods stimulate secondary metabolism while reducing adaptive growth attenuation. Plant Cell Environ 42:801–814.

Holub P, Nezval J, Štroch M et al (2019) Induction of phenolic compounds by UV and PAR is modulated by leaf ontogeny and barley genotype. Plant Physiol Biochem 134:81–93.

Ishida M, Hara M, Fukino N et al (2014) Glucosinolate metabolism, functionality and breeding for the improvement of *Brassicaceae* vegetables. Breed Sci. 64:48–59

Jansen MAK (2002) Ultraviolet-B radiation effects on plants: Induction of morphogenic responses. Physiol Plant 116:423–429.

Jenkins GI (2009) Signal transduction in responses to UV-B radiation. Annu Rev Plant Biol 60:407–431.

Kanojia A, Gupta S, Benina M et al (2020) Developmentally controlled changes during *Arabidopsis* leaf development indicate causes for loss of stress tolerance with age. J Exp Bot 71:6340–6354.

Kim D, Kang WH, Hwang I et al (2020a) Use of structurally-accurate 3D plant models for estimating light interception and photosynthesis of sweet pepper (*Capsicum annuum*) plants. Comput Electron Agric 177:105689.

Kim J, Kang WH, Son JE (2020b) Interpretation and evaluation of electrical lighting in plant factories with ray-tracing simulation and 3D plant modeling. Agronomy 10:1545.

Konishi A, Eguchi A, Hosoi F, Omasa K (2009) 3D monitoring spatio-temporal effects of herbicide on a whole plant using combined range and chlorophyll a fluorescence imaging. Funct Plant Biol 36:874–879.

Kozai BTK (2013) Resource use efficiency of closed plant production system with artificial light : Concept, estimation and application to plant factory. Proc Jpn Acad Ser B Phys Biol Sci 89:447–461.

Krumbein A, Schonhof I, Smetanska I et al (2010) Improving levels of bioactive compounds in *Brassica* vegetables by crop management strategies. Acta Hortic 856:37–48.

Lee MJ, Lim S, Kim J, Oh MM (2012) Heat shock treatments induce the accumulation of phytochemicals in kale sprouts. Korean J Hortic Sci Technol 30:509–518.

Lee M, Son JE, Oh MM (2013) Growth and phenolic content of sowthistle grown in a closed-type plant production system with a UV-A or UV-B lamp. Hortic Environ Biotechnol 54:492–500.

Liakoura V, Bornman JF, Karabourniotis G (2003) The ability of abaxial and adaxial epidermis of sun and shade leaves to attenuate UV-A and UV-B radiation in relation to the UV absorbing capacity of the whole leaf methanolic extracts. Physiol Plant 117:33–34.

Linić I, Šamec D, Grúz J et al (2019) Involvement of phenolic acids in short-term adaptation to salinity stress is species-specific among *Brassicaceae*. Plants 8:155.

Liu T, Pan Y, Lu Z et al (2020) Canopy light and nitrogen distribution are closely related to nitrogen allocation within leaves in *Brassica napa* L. F Crop Res 258:107958.

Lois R (1994) Accumulation of UV-absorbing flavonoids induced by UV-B radiation in *Ambidopsis thaliana* L. Planta 194:498–503.

Majer P, Hideg É (2012) Developmental stage is an important factor that determines the antioxidant responses of young and old grapevine leaves under UV irradiation in a green-house. Plant Physiol Biochem 50:15–23.

Martínez-Lüscher J, Brillante L, Kurtural SK (2019) Flavonol profile is a reliable indicator to assess canopy architecture and the exposure of red wine grapes to solar radiation. Front Plant Sci 10.

Martínez-lüscher J, Morales F, Delrot S et al (2013) Short- and long-term physiological responses of grapevine leaves to UV-B radiation. Plant Sci 213:114–122.

McKenzie R, Connor B, Bodeker G (1999) Increased summertime UV radiation in new zealand in response to ozone Loss. Science 285:1709–1711.

Meyer S, Louis J, Moise N et al (2009) Developmental changes in spatial distribution of in vivo fluorescence and epidermal UV absorbance over *Quercus petraea* leaves. Ann Bot 104:621–633.

Morales LO, Tegelberg R, Brosché M et al (2011) Temporal variation in epidermal flavonoids due to altered solar UV radiation is moderated by the leaf position in *Betula pendula*. Physiol Plant 143:261–270.

Moreira-Rodríguez M, Nair V, Benavides J et al (2017) UVA, UVB light doses and harvesting time differentially tailor glucosinolate and phenolic profiles in broccoli sprouts. Molecules 22:1065.

Mosadegh H, Trivellini A, Ferrante A et al (2018) Applications of UV-B lighting to enhance phenolic accumulation of sweet basil. Sci Hortic (Amsterdam) 229:107–116.

Mosadegh H, Trivellini A, Lucchesini M et al (2019) UV-B physiological changes under conditions of distress and eustress in sweet basil. Plants 8:396.

Moustaka J, Tanou G, Adamakis ID et al (2015) Leaf age-dependent photoprotective and antioxidative response mechanisms to paraquat-induced oxidative stress in *Arabidopsis thaliana*. Int J Mol Sci 16:13989–14006.

Neugart S, Schreiner M (2018) UVB and UVA as eustressors in horticultural and agricultural crops. Sci Hortic (Amsterdam) 234:370–381.

Neugart S, Zietz M, Schreiner M et al (2012) Structurally different flavonol glycosides and hydroxycinnamic acid derivatives respond differently to moderate UV-B radiation exposure. Physiol Plant 145:582–593.

Oh MM, Trick HN, Rajashekar CB (2009) Secondary metabolism and antioxidants are involved in environmental adaptation and stress tolerance in lettuce. J Plant Physiol 166:180–191.

Olsen H, Aaby K, Borge GIA (2009) Characterization and quantification of flavonoids and hydroxycinnamic acids in curly kale (*Brassica oleracea* L. Convar. *acephala* Var. *sabellica*) by HPLC-DAD-ESI-MS[n]. J Agric Food Chem 57:2816–2825.

Parihar P, Singh S, Singh R et al (2015) Changing scenario in plant UV-B research:UV-B from a generic stressor to a specific regulator. J. Photochem. Photobiol. B Biol. 153:334–343

Podda A, Pollastri S, Bartolini P et al (2019) Drought stress modulates secondary metabolites in *Brassica oleracea* L. convar. *acephala* (DC) Alef, var. *sabellica* L. J Sci Food Agric 99:5533–5540.

Podsędek A (2007) Natural antioxidants and antioxidant capacity of *Brassica* vegetables: A review. LWT - Food Sci Technol 40:1–11.

Portes TDA, Melo HC De (2014) Light interception, leaf area and biomass production as a function of the density of maize plants analyzed using mathematical models. Acta Sci Agron 17892:457–463.

Radušienė J, Karpavičienė B, Stanius Ž (2013) Effect of external and internal factors on secondary metabolites accumulation in St. John's Worth. Bot Lith 18:101–108.

Ramakrishna A, Ravishankar GA (2011) Influence of abiotic stress signals on secondary metabolites in plants. Plant Signal Behav 6:1720–1731.

Rapacz M (2007) Chlorophyll a fluorescence transient during freezing and recovery in winter wheat. Photosynthetica 45:409–418.

Reifenrath K, Müller C (2007) Species-specific and leaf-age dependent effects of ultraviolet radiation on two *Brassicaceae*. Phytochemistry 68:875–885.

Šamec D, Urlić B, Salopek-Sondi B (2019) Kale (*Brassica oleracea* var. *acephala*) as a superfood: Review of the scientific evidence behind the statement. Crit Rev Food Sci Nutr 59:2411–2422.

Sarlikioti V, De Visser PHB, Marcelis LFM (2011) Exploring the spatial distribution of light interception and photosynthesis of canopies by means of a functional–structural plant model. Ann Bot 107:875–883.

Sperdouli I, Moustakas M (2014a) A better energy allocation of absorbed light in photosystem II and less photooxidative damage contribute to

acclimation of *Arabidopsis thaliana* young leaves to water deficit. J Plant Physiol 171:587–593.

Sperdouli I, Moustakas M (2014b) Leaf developmental stage modulates metabolite accumulation and photosynthesis contributing to acclimation of *Arabidopsis thaliana* to water deficit. 127:481–489.

Stewart DW, Costa C, Dwyer LM et al (2003) Canopy Structure, light interception, and photosynthesis in maize. Agron J 95:1465–1474.

Strauss S, Lempe J, Prusinkiewicz P et al (2020) Phyllotaxis: Is the golden angle optimal for light capture? New Phytol 225:499–510.

Toscano S, Trivellini A, Cocetta G et al (2019) Effect of preharvest abiotic stresses on the accumulation of bioactive compounds in horticultural produce. Front Plant Sci 10:1–17.

Vos J, Evers JB, Andrieu   et al (2010) Functional–structural plant modelling : A new versatile tool in crop science. J Exp Bot 61:2101–2115.

Walsh RP, Bartlett H, Eperjesi F (2015) Variation in carotenoid content of kale and other vegetables: A review of pre- and post-harvest effects. J Agric Food Chem 63:9677–9682.

Xu P, Su H, Jin R et al (2020) Shading effects on leaf color conversion and biosynthesis of the major secondary metabolites in the albino tea cultivar "Yujinxiang". J Agric Food Chem 68:2528–2538

Xue H, Han Y, Li Y et al (2015) Spatial distribution of light interception by different plant population densities and its relationship with yield. F Crop Res 184:17–27.

Yang X, Miller DR, Montgomery ME (1993) Vertical distributions of canopy foliage and biologically active radiation in a defoliated/refoliated hardwood forest. Agric For Meteorol 67:129–146.

Yavaş İ, Ünay A, Ali S, Abbas Z (2020) UV-B radiations and secondary metabolites. Turkish J Agric Sci Technol 8:147–157

Yoon HI, Kim D, Son JE (2020) Spatial and temporal bioactive compound contents and chlorophyll fluorescence of kale (*Brassica oleracea* L.) under UV-B exposure near harvest time in controlled environments. Photochem Photobiol 96:845–852.

Yoon HI, Kim JS, Kim D et al (2019) Harvest strategies to maximize the annual production of bioactive compounds, glucosinolates, and total antioxidant activities of kale in plant factories. Hortic Environ Biotechnol 60:883–894.

Zhao B, Wang L, Pang S et al (2020) UV-B promotes flavonoid synthesis in Ginkgo biloba leaves. Ind Crop Prod 151:112483.

Zietz M, Weckmüller A, Schmidt S et al (2010) Genotypic and climatic influence on the antioxidant activity of flavonoids in kale (*Brassica oleracea* var. *sabellica*). J Agric Food Chem 58:2123–2130.

ABSTRACT IN KOREAN

UV−B 광 에너지는 식물의 생활성 화합물을 효율적으로 축적시키기 위한 수단으로써 식물공장에서 흔히 사용된다. 그러나 생육진전에 따른 식물 구조의 변화는 엽 위치별 수광 분포를 다르게 하므로 UV−B 광에 의한 생활성 화합물의 생성 효과를 정확히 평가하기 어렵다. 본 연구의 목적은 케일의 생육 진전이 UV−B 수광, 생활성 화합물의 위치적 분포와 두 관계에 주는 영향을 정량적으로 분석하는 것이다. 케일은 광합성 광량자속밀도 $200\,\mu\mathrm{mol}\cdot\mathrm{m}^{-2}\cdot\mathrm{s}^{-1}$, 광주기 16 시간인 식물공장에서 자랐고, 정식 후 14 일과 정식 후 28 일에 수확되었다. 케일은 수확 전 1 일, 2 일, 3 일 동안 두 가지 수준의 UV−B (1.3 W m^{-2}, 하루 6 시간 혹은 12 시간)로 조사되었다. 개체 내의 상, 중, 하단부 엽에 대한 UV−B 수광, 총 플라보노이드 함량(TFC), 총 페놀함량(TPC)이 측정되었다. 공간적 UV−B 수광은 3 차원 식물모델과 광 추적 시뮬레이션을 통해 분석되었다. 본 연구의 UV−B 수준은 엽면적, 잎의 생체중과 건물중을 포함한 생육에 영향을 주지 않았다. 생육이 진전되면서, 상단부 엽의 수광은 중단부 엽과 하단부 엽에 비해 각각 34.1%, 88.8% 높았다. 상단부 엽의 생활성 화합물은 중단부

엽과 하단부 엽에 비해 각각 29.3–36.8%, 70.1–82.6% 높았다. 중단부 UV−B 누적 흡수된 UV−B 광량에 대한 TFC 의 증가율은 상단부에서, TPC 의 증가율은 중단부에서 가장 높았다. 동일한 UV−B 광 수준에서도 케일의 UV−B 수광과 감수성은 엽 위치와 생육단계에 따라 차이가 있었고 이는 생활성 화합물의 생합성에 영향을 주었다. 본 방법은 추후 UV−B 광을 사용한 식물공장 내 이차대사산물 생산량 추정 및 정량화에 기여할 것으로 기대된다.

추가 주요어: 수직 농장, 식물 구조, 엽 위치, 페놀 함량, 3 차원 분석, UV 수율

학 번: 2019−21562